A NOVEL RECIPROCAL SOUND TRANSMISSION MEASURING METHOD, APPLIED ON A COMPOSITE FUSELAGE

Henk van der Wal*, Pieter Sijtsma*, Benoit Berton, Pierre Hardy****
***National Aerospace Laboratory NLR, ****Dassault Aviation**

Keywords: *Cabin noise, Fuselage wall, Reciprocal sound transmission measuring method, Nearfield acoustic holography, Sound intensity*

Abstract

In the framework of the 5th FP EU project FACE (Friendly Aircraft Cabin Environment), NLR, in consultation with Dassault, have performed sound transmission tests on a composite fuselage barrel, using two different methods. The first method is a reciprocal technique, i.e. measuring the volume velocity of a source inside the barrel, and measure also the volume velocity outside the barrel. The second method applies intensity measurements on the barrel exterior, exciting the barrel interior with the same sound source, measuring also the average sound pressure inside the barrel.

The most important parameter governing the barrel TL is the ring frequency. Measured and predicted values of the ring frequency agreed well. The TL (Transmission Loss) showed a minimum at the ring frequency, and increased above this frequency according to the mass law.

The reciprocal technique appeared to work well. Sound intensity results obtained with the traversed microphone array agreed very well with results of the intensity measurements.

1 Introduction

In this age of monotonic increasing fuel prices, fuel saving becomes more and more important. For aeroplanes, saving of mass is a tried and tested method for fuel saving. One promising method for mass reduction is replacing the metal aircraft fuselage by a composite one. Due to its reduced mass however, an important issue for composite fuselages is to suppress the increased noise transmission into the cabin.

For a given fuselage, the expected in-flight cabin noise levels can be determined from the exterior in-flight fuselage pressure distribution and a set of measured transfer functions (exterior to interior sound pressure on specific points). The set of transfer functions can also be used for validation of numerical tools for the prediction of sound transmission through the fuselage. These types of tools are presently being developed by aircraft manufacturers for optimization of the fuselage structure. The transfer functions can be measured directly by point excitation with an exterior sound source which is, however, a rather complicated procedure. Much easier is to determine these transfer functions with a reciprocal technique, using a sound source in the cabin and measuring volume velocities (or an equivalent parameter) instead of sound pressures. Mason and Fahy [1], [2] developed such a reciprocal technique, using a capacitive transducer for the volume velocity measurement at the fuselage surface. MacMartin [3] applied this method on a deHavilland Dash-8 aircraft.

The present paper describes a similar method, however determining the normal pressure derivative at the fuselage wall with an alternative technique, namely a NAH reconstruction (Nearfield Acoustic Holography) on the sound pressures, measured on a grid close to the fuselage barrel. For the reconstruction procedure, the method of Williams [4] has been adopted.

It is noted that the complete sound field between the measuring plane and the barrel can be reconstructed with the NAH procedure. Consequently, also the TL according to ISO

15186 [5] can be determined from the measured array data and the average sound pressure, measured inside the barrel.

With this point-to-point transfer function concept it is possible to focus on specific ("passenger's ear") positions in the cabin, and to assess both the influence of weak spots in the fuselage wall (i.e. with a reduced TL) and the effect of a realistic (in flight) excitation on the sound pressure at a specific interior position. With a conventional TL measuring method (based on ISO 15186 [5]) it is much more complicated, inaccurate or impossible to assess the effect of in flight excitation.

Fig. 1. FUBACOMP barrel with acoustic array

Within the EU project FACE (Friendly Aircraft Cabin Environment) noise transmission tests have been performed by NLR, in consultation with Dassault, on the FUBACOMP barrel, see Fig. 1. This business jet type fuselage barrel consists of a composite honeycomb structure without frames and stiffeners. The tests have been performed in June 2006. The goal of the measurements was to provide experimental data for validation of numerical predictions, to be performed by Dassault. Moreover, the measured TL data of the FUBACOMP barrel, determined both with the reciprocal technique and from sound intensity measurements, have been compared with TL data, measured by Dassault on a flat panel with the same structure.

In the present paper the experimental methods, set-up and results are described for the reciprocal and conventional TL measurements on the FUBACOMP barrel.

2 Experimental Methods

2.1 Reciprocal and NAH Techniques

For the reciprocal method, the barrel volume is excited with a monopole source with a known source strength q, as determined from the electrical input V_{ref}. For this, the sound source has been calibrated in an anechoic room. The pressure normal derivative $\partial p/\partial n$ of the exterior barrel surface is determined from measurements close to the barrel surface with a traversing microphone array. The TL-measurements are based on Lyamshev's principle of reciprocity [6], which states that the following transmissions are equivalent:

- from a point force (f_1) exciting a given point A on the outer wall of the barrel to sound pressure (p_1) on a given point B inside the barrel,
- from a monopole source (source strength q_2) at point B inside the barrel to pressure normal derivative $\partial p_2/\partial n$ on the outer wall at point A.

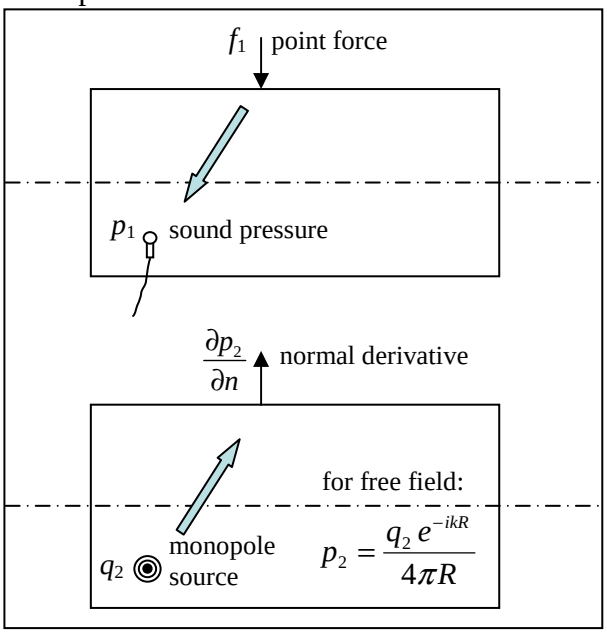

Fig. 2. Lyamshev's principle of reciprocity

This principle is illustrated in Fig. 2. In summary, we have $p_1 / f_1 = (-\partial p_2/\partial n)/q_2$. The aim of the method is to determine the transfer function $TF(p_1) = p_1 / f_1$ which is, according to the equivalent transmissions described above, equal to the transfer function $TF(q_2) = (-\partial p_2 / \partial n)/q_2$. The transfer function $TF(q_2)$ is evaluated by cross-correlating with the input voltage signal V_{ref} to the dodecahedron loudspeaker:

$$\frac{-\frac{\partial p}{\partial n}}{q} = \frac{-\left\langle \frac{\partial p}{\partial n} V_{ref}^{*} \right\rangle \Big/ \left\| V_{ref} \right\|^2}{\left\langle q V_{ref}^{*} \right\rangle \Big/ \left\| V_{ref} \right\|^2} \qquad (1)$$

For the denominator, results from the earlier source calibration measurements have been used. Furthermore, a reciprocal TL value, based on the monopole source strength q and pressure normal derivative, and indicated with TL_R, can be determined from the transfer function $TF(q)$: $TL_R = -20 \log \left| TF(q) \cdot S_{ref} \right|$, with S_{ref} = 1 m^2 a reference surface. The theoretical background of reciprocity is described in sections 2.2, 2.3 and 2.4.

A measurement for one source position yields $TF(q_2)$ transfer functions from the source position to all arbitrary points on the outside surface of the fuselage, located inside the barrel portion, covered by the measuring surface. If data are desired for more positions inside and outside the barrel, measurements with different positions of the source and measuring surface respectively are necessary.

The exterior sound field near the barrel, including the pressure normal derivative at the barrel surface, has been reconstructed from sound pressure measurements close to the fuselage on an equidistant cylindrical grid of 64×64 positions over a quarter of the fuselage barrel circumference (grid point spacing Δ_m), using NAH (Nearfield Acoustic Holography).

The reconstruction procedure for the distribution of the sound pressure and its normal derivative at the fuselage surface is described by Williams [4]. For this calculation procedure, the following has been assumed:

- cylindrical geometry of barrel and measuring grid (covering a quarter of the cylinder circumference),
- in circumferential direction, a part equal to C/N (with C the circumference and N an integer) of the circumference is covered with microphones,
- the number of microphone positions in circumferential direction is 2^{M_c}, with M_c an integer,
- in axial direction, the number of microphone positions is 2^{M_a}, with M_a also an integer,
- at the cylindrical measuring grid, the sound from outside this cylinder (e.g. from reflections at walls), is negligible compared to the sound radiated directly from the barrel. Also, the sound, radiated by the portion of the cylinder, not covered by the array has been neglected. Therefore, the results at the 3 outermost grid lines (having distances of $\Delta_m/2$, $3\Delta_m/2$ and $5\Delta_m/2$ to the measuring surface boundary) may be inaccurate,
- the monopole source has a uniform directivity.

The pressure normal derivative on the outer wall of the barrel is obtained from microphone measurements on a cylindrical grid at a short distance, by using NAH. This process involves the following 5 steps:

Step1: Measure the sound pressure p at $r = r_1$.

Step2: Perform a Fourier transform in two directions: $p(r_1, x, \theta) \rightarrow \hat{p}(r_1, \alpha, m)$.

Step3: Transform the sound field from $r = r_1$ to $r = r_2$:

$$\frac{\mathrm{d}\,\hat{p}}{\mathrm{d}\,r}(r_2, \alpha, m) = \hat{p}(r_1, \alpha, m) \gamma H_m^{(2)\prime}(\gamma r_2) \Big/ H_m^{(2)}(\gamma r_1),$$

where $\gamma = \sqrt{k^2 - \alpha^2}$, $H_m^{(2)}$ are Hankel functions of the second kind, and $'$ denotes derivative.

Step4: Multiply $\mathrm{d}\,\hat{p}/\mathrm{d}\,r$ with an appropriate filter function for suppression of measurement noise for large wave numbers.

Step5: Perform the inverse Fourier transform: $\frac{\mathrm{d}\,\hat{p}}{\mathrm{d}\,r}(r_2,\alpha,m) \rightarrow \frac{\partial p}{\partial n}(r_2,x,\theta)$.

The method, described above, applies to a cylindrical geometry. Consequently, the method is only suited for the cylindrical (rear) part of the FUBACOMP barrel. In the sections 2.5 and 2.6 the mathematical foundation for the calculation procedure of sound pressure at the fuselage surface, its normal derivative and the sound intensity, from the measured raw data is described. NAH may also be applied to plane or spherical surfaces [4].

2.2 Reciprocity of an Elastic Body

Let A be an elastic body with boundary S and outwardly directed normal vector $\vec{n}$. Suppose there are external forces acting on A: $-f(\vec{x})\vec{n}(\vec{x}),\ \vec{x}\in S$. As a result A will be deformed, featuring a surface displacement w in the direction of $\vec{n}$. This surface displacement w can be interpreted as an operator from the function space $S \rightarrow \mathbf{R}$ to itself. This can be written as:

$$w[f] \text{ or } w[f(\cdot)](\vec{x}). \tag{2}$$

We assume the following:

1. f and w are small.
2. w depends linearly on f.
3. There is reciprocity: Suppose w_1 is the displacement due to a unit point source acting on $\vec{x}_1$, and w_2 is due to a unit point source in $\vec{x}_2$, then $w_1(\vec{x}_2) = w_2(\vec{x}_1)$.

We can write assumption 3, analogously to Eq. (2), as:

$$w[\delta(\cdot - x_1)](\vec{x}_2) = w[\delta(\cdot - x_2)](\vec{x}_1) \tag{3}$$

where δ is the Dirac-delta function. Now suppose that w_1 is the displacement due to a force field f_1, and that w_2 is induced by f_2. Then we can prove:

$$\iint_S \left(w_1(\vec{x})\, f_2(\vec{x}) - w_2(\vec{x})\, f_1(\vec{x})\right) dS(\vec{x}) = 0 \tag{4}$$

It is noted that (4) also holds for time-dependent f and w, or if they are Fourier-transformed.

2.3 Lyamshev's Principle of Reciprocity

In this section, a brief derivation is given of Lyamshev's principle of reciprocity [6]. We start from the Helmholtz equation for the acoustic pressure p:

$$\nabla^2 p + k^2 p = 0 \tag{5}$$

where $k = \omega/c$ is the Helmholtz number, ω the angular frequency and c the sound speed. Suppose p_1 is the acoustic pressure field due to a point source in $\vec{x}_1$, in other words:

$$\nabla^2 p_1(\vec{x}) + k^2 p_1(\vec{x}) = -q_1 \delta(\vec{x} - \vec{x}_1) \tag{6}$$

where q_1 is the source strength. An elastic body A will be deformed due to acoustic pressures acting on the surface S, say:

$$w_1 = w[p_1] \tag{7}$$

Suppose that p_2 is the acoustic pressure field due to an external force field acting on S (e.g. the diffracted field due to an incoming pressure field). Hence, for p_2 we have:

$$\nabla^2 p_2(\vec{x}) + k^2 p_2(\vec{x}) = 0 \tag{8}$$

$$w_2 = w[p_2 + f_2] \tag{9}$$

By multiplying (6) with $p_2(\vec{x})$, and (8) with $p_1(\vec{x})$, and subtracting the results, we find:

$$\begin{aligned} &q_1 p_2(\vec{x})\delta(\vec{x} - \vec{x}_1) \\ &= p_1(\vec{x})\nabla^2 p_2(\vec{x}) - p_2(\vec{x})\nabla^2 p_1(\vec{x}) \end{aligned} \tag{10}$$

Integrating this over $\mathbf{R}^3 \setminus A$, we obtain:

$$\begin{aligned} q_1 p_2(\vec{x}_1) &= \iiint_{\mathbf{R}^3\setminus A} q_1 p_2(\vec{x})\delta(\vec{x} - \vec{x}_1)\,d\vec{x} \\ &= \iiint_{\mathbf{R}^3\setminus A} \left(p_1(\vec{x})\nabla^2 p_2(\vec{x}) - p_2(\vec{x})\nabla^2 p_1(\vec{x})\right) d\vec{x} \\ &= \iiint_{\mathbf{R}^3\setminus A} \nabla\cdot\left(p_1(\vec{x})\nabla p_2(\vec{x}) - p_2(\vec{x})\nabla p_1(\vec{x})\right) d\vec{x} \\ &= -\iint_S \left(p_1(\vec{x})\frac{\partial p_2}{\partial n}(\vec{x}) - p_2(\vec{x})\frac{\partial p_1}{\partial n}(\vec{x})\right) dS(\vec{x}). \end{aligned} \tag{11}$$

The minus sign in (11) is due to the direction of $\vec{n}$, pointing into $\mathbf{R}^3 \setminus A$. The relation between $\frac{\partial p}{\partial n}$ and w is:

$$-\rho_0 \omega^2 w + \frac{\partial p}{\partial n} = 0, \tag{12}$$

where ρ_0 is the air density. This follows from the impulse equation $\rho_0 \partial \vec{v}/\partial t + \nabla p = 0$, together with $\vec{v} \cdot \vec{n} = \partial w/\partial t$ and $\partial/\partial t = i\omega$. With (12), we can evaluate (11) further as:

$$q_1 p_2(\vec{x}_1) = -\rho_0 \omega^2 \iint_S \left(p_1(\vec{x}) w_2(\vec{x}) - p_2(\vec{x}) w_1(\vec{x}) \right) dS(\vec{x}). \tag{13}$$

With (7), (9) and (4) we can write:

$$\begin{aligned} q_1 p_2(\vec{x}_1) &= -\rho_0 \omega^2 \iint_S \left(p_1 w_2 - p_2 w_1 \right) dS \\ &= -\rho_0 \omega^2 \iint_S \left(p_1 w[p_2 + f_2] - p_2 w[p_1] \right) dS \\ &= -\rho_0 \omega^2 \iint_S \left((p_2 + f_2) w[p_1] - p_2 w[p_1] \right) dS \\ &= -\rho_0 \omega^2 \iint_S f_2 w[p_1] dS = -\iint_S f_2 \frac{\partial p_1}{\partial n} dS. \end{aligned} \tag{14}$$

If f_2 is a force acting on a unit surface around $\vec{\xi}_2 \in S$, we have

$$q_1 p_2(\vec{x}_1) = -f_2 \frac{\partial p_1}{\partial n}(\vec{\xi}_2) \tag{15}$$

This can also be written as:

$$p_2(\vec{x}_1)/f_2 = -\frac{\partial p_1}{\partial n}(\vec{\xi}_2) \Big/ q_1 \tag{16}$$

In other words, the transfer function $f_2 \to p_2(\vec{x}_1)$ is the same as $q_1 \to -\frac{\partial p_1}{\partial n}(\vec{\xi}_2)$.

2.4 Application to Fuselage Barrel

External forces f acting on a fuselage can be due to the turbulent boundary layer, or to an (undisturbed) incoming acoustic field. In both cases, it is of interest what the induced acoustic pressures are inside the fuselage. We can write these formally as:

$$p(\vec{x}) = \iint_S f(\vec{\xi}) T(\vec{x}, \vec{\xi}) dS(\vec{\xi}) \tag{17}$$

where $T(\vec{x}, \vec{\xi})$ is the transfer function from $f(\vec{\xi})$ to $p(\vec{x})$. According to (16), we can calculate $T(\vec{x}, \vec{\xi})$ as:

$$T(\vec{x}, \vec{\xi}) = -\frac{\partial p}{\partial n}(\vec{\xi}) \Big/ q(\vec{x}) \tag{18}$$

where $q(\vec{x})$ is the known strength of a point source in $\vec{x}$, and $\partial p/\partial n(\vec{\xi})$ are normal velocities measured on the fuselage.

2.5 STSF in Cylindrical Co-ordinates

In the following, the STSF procedure (Spatial Transformation of Sound Fields) is described. The Helmholtz equation for the acoustic pressure reads:

$$\nabla^2 p + k^2 p = 0 \tag{19}$$

where $k = \omega/c$ is the Helmholtz number, ω the angular frequency and c the sound speed. In a cylindrical co-ordinate system (x, r, θ), Eq. (19) transforms into

$$\frac{\partial^2 p}{\partial x^2} + \frac{1}{r}\frac{\partial}{\partial r}\left(r \frac{\partial p}{\partial r} \right) + \frac{1}{r^2}\frac{\partial^2 p}{\partial \theta^2} + k^2 p = 0. \tag{20}$$

We express p as the summation:

$$\begin{aligned} p(x, r, \theta) &= \sum_{m=-M/2+1}^{m=M/2-1} p_m(x, r) e^{i\vartheta_m \theta}, \\ \vartheta_m &= 2\pi m / M\Delta\theta \end{aligned} \tag{21}$$

where M is the number of microphones in circumferential direction and $\Delta\theta$ the spacing. If the microphones span the full circumference, then $M\Delta\theta = 2\pi$, and thus $\vartheta_m = m$. If the microphones span, say, 90 degrees, then $M\Delta\theta = 0.5\pi$, and thus $\vartheta_m = 4m$. For (21) we obtain:

$$\frac{\partial^2 p_m}{\partial x^2} + \frac{1}{r}\frac{\partial}{\partial r}\left(r \frac{\partial p_m}{\partial r} \right) - \frac{\vartheta_m^2}{r^2} p + k^2 p = 0. \tag{22}$$

Next, the Fourier transform $x \to \alpha$ is performed:

$$p_m(x,r)=\sum_{n=-N/2+1}^{N/2-1} p_{m,n}(r)e^{i\alpha_n x},$$
$$\alpha_n = 2\pi n/N\Delta x \tag{23}$$

where N is the number of microphone positions and Δx the spacing. Thus, we obtain:

$$\frac{1}{r}\frac{d}{dr}\left(r\frac{dp_{m,n}}{dr}\right)+\left(k^2-\alpha_n{}^2-\frac{\vartheta_m^2}{r^2}\right)p=0. \tag{24}$$

The general solution of (24), satisfying the Sommerfeld condition, is

$$p_{m,n}(r)=A_{m,n}H^{(2)}_{\vartheta_m}(\gamma_n r) \tag{25}$$

where $H^{(2)}_{\vartheta_m}$ is the ϑ_m-th order Hankel function of the second kind, and

$$\gamma_n=\begin{cases} k\sqrt{1-\alpha_n^2/k^2}, & \alpha_n^2<k^2,\\ -i\sqrt{\alpha_n^2-k^2}, & \alpha_n^2\geq k^2. \end{cases} \tag{26}$$

Suppose that the acoustic pressure field is known on a cylinder with $r=a$. Then, using (25), the pressure field can be calculated elsewhere:

$$p_{m,n}(r)=p_{m,n}(a)\,H^{(2)}_{\vartheta_m}(\gamma_n r)\Big/H^{(2)}_{\vartheta_m}(\gamma_n a) \tag{27}$$

Likewise, we have for the radial derivative:

$$\frac{dp_{m,n}}{dr}(r)=p_{m,n}(a)\frac{\partial}{\partial r}H^{(2)}_{\vartheta_m}(\gamma_n r)\Big/H^{(2)}_{\vartheta_m}(\gamma_n a) \tag{28}$$

2.6 Spatial Filter

In the following, the STSF procedure (Spatial Transformation of Sound Fields) is described. If $|r-a|<<r$, then:

$$H^{(2)}_{\vartheta_m}(\gamma_n r)\approx e^{-i\mu_{m,n}(r-a)}H^{(2)}_{\vartheta_m}(\gamma_n a) \tag{29}$$

with:

$$\mu_{m,n}=\begin{cases} k\sqrt{1-\left(\alpha_n^2+\vartheta_m^2/a^2\right)^2/k^2}, \\ \quad \text{for } \alpha_n^2+\vartheta_m^2/a^2<k^2, \\ -i\sqrt{\alpha_n^2+\vartheta_m^2/a^2-k^2}, \\ \quad \text{for } \alpha_n^2+\vartheta_m^2/a^2\geq k^2. \end{cases} \tag{30}$$

Consequently, we have

$$\frac{\partial}{\partial r}H^{(2)}_{\vartheta_m}(\gamma_n r)\approx -i\mu_{m,n}e^{-i\mu_{m,n}(r-a)}H^{(2)}_{\vartheta_m}(\gamma_n a) \tag{31}$$

Hence, we have for (27) and (28):

$$p_{m,n}(r)\approx p_{m,n}(a)e^{-i\mu_{m,n}(r-a)} \tag{32}$$

$$\frac{dp_{m,n}}{dr}(r)\approx -i\mu_{m,n}p_{m,n}(a)e^{-i\mu_{m,n}(r-a)} \tag{33}$$

For large values of $\alpha_n^2+\vartheta_m^2/a^2$, in other words, for short wave lengths, we have:

$$\exp\left(-i\mu_{m,n}(r-a)\right)=$$
$$\exp\left(-(r-a)\sqrt{\alpha_n^2+\vartheta_m^2/a^2-k^2}\right) \tag{34}$$

For $r>a$, there is an exponential decay of short wave lengths, but for $r<a$, there is an exponential increase, which leads to instability. The amplifications of short wave lengths are:

$$A_1\left(k^2,\alpha_n^2+\vartheta_m^2/a^2\right)=\left|p_{m,n}(r)/p_{m,n}(a)\right|$$
$$\approx\exp\left[\delta\sqrt{\alpha_n^2+\vartheta_m^2/a^2-k^2}\right] \tag{35}$$

$$A_2\left(k^2,\alpha_n^2+\vartheta_m^2/a^2\right)=\left|\frac{dp_{m,n}}{dr}(r)\Big/p_{m,n}(a)\right|\approx$$
$$\sqrt{\alpha_n^2+\vartheta_m^2/a^2-k^2}$$
$$\times\exp\left[\delta\sqrt{\alpha_n^2+\vartheta_m^2/a^2-k^2}\right] \tag{36}$$

where

$$\delta=a-r \tag{37}$$

Instabilities can be avoided by applying a filter, i.e., by replacing (27) and (28) by:

$$p_{m,n}(r)=\Phi\left(k^2,\alpha_n^2+\vartheta_m^2/a^2\right)$$
$$\times p_{m,n}(a)\,H^2_{\vartheta_m}(\gamma_n r)\Big/H^2_{\vartheta_m}(\gamma_n a) \tag{38}$$

$$\frac{dp_{m,n}}{dr}(r)=\Phi\left(k^2,\alpha_n^2+\vartheta_m^2/a^2\right)$$
$$\times p_{m,n}(a)\frac{\partial}{\partial r}H^2_{\vartheta_m}(\gamma_n r)\Big/H^2_{\vartheta_m}(\gamma_n a) \tag{39}$$

where Φ is the filter function. We applied a simple filter:

$$\Phi(k^2,\zeta^2)=\begin{cases}1, & \zeta^2 \le k_c^2,\\ 0, & \zeta^2 > k_c^2.\end{cases} \quad (40)$$

For the cut-off number k_c we will choose

$$k_c = k + \Delta k \quad (41)$$

where Δk is independent of frequency. The maximum amplifications after application of the filter are:

$$A_1\left(k^2,k_c^2\right)=\exp\left[\delta\sqrt{k_c^2-k^2}\right] \quad (42)$$

$$A_2\left(k^2,k_c^2\right)=\sqrt{k_c^2-k^2}\exp\left[\delta\sqrt{k_c^2-k^2}\right] \quad (43)$$

If A_2 becomes larger than a prescribed maximum amplification λ, then k_c is decreased until $A_2\left(k^2,k_c^2\right)=\lambda$.

Finally, the sound intensity is calculated from

$$I_{m,n}=\mathrm{Re}\left[-\frac{i\,p_{m,n}}{2k\rho_0 c}\left(\frac{\partial p_{m,n}}{\partial r}\right)^*\right] \quad (44)$$

with * denoting complex conjugate.

2.7 Sound Intensity and TL

The TL has been measured according to ISO 15186(2) [5]. For this, the barrel has been excited with the sound source, used also for the reciprocal measurements. The average sound pressure level inside the barrel has been measured, and sound intensity measurements have been performed on the part of the exterior fuselage surface, coinciding with the surface, corresponding with the measuring grid for the reciprocal measurements. As a validation of the NAH procedure, the exterior sound intensity has been calculated from the array data as well, and the corresponding TL data have been compared with the TL data, determined from the direct sound intensity measurements.

3 Test set-up and test procedures

The test set-up consisted of a sound source (see Fig. 3) inside and a circular line-array of 64 equidistant microphones outside the barrel. The source has been successively placed on two positions. The signal generator output voltage (band limited random noise, 0-6 kHz), fed into the source, has been measured simultaneously with the microphone array signals.

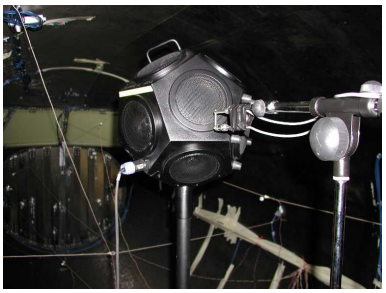

Fig. 3. Volume velocity source (B&K4296 "OmniPower")

The distance Δ_m between the microphones, located on a circle, 27 mm from the barrel surface, was 25 mm, so as to match a measuring surface, equal to a quarter of the barrel circumference (-25° and +63° with respect to the vertical plane through the barrel axis (array position as depicted in Fig. 1). This position of the array was selected in order to suppress the effect of reflections by objects close to the barrel. By this choice however, the measurement surface did not include the door and windows. The disadvantage of not measuring these parts was acceptable, as the designs of these parts were not representative for aircraft structures. The line-array of 64 microphones has been traversed in axial direction over the available traverse trajectory (2.3 m in front of the grey plate at the rear of the barrel, see Fig. 1), corresponding with 89 array positions), the increment of 25 mm being equal to the microphone spacing. This facilitates post processing over different areas, each corresponding with 64×64 microphone positions.

For the lowest frequency of interest (700 Hz), the length of a quarter of the circumference is larger than three times the wavelength (in air). For a microphone spacing of 25 mm, the maximum frequency (Δ_m less than half a wavelength) is above 6 kHz.

The block size has been set to 32768 (equal to the sample frequency in Hz), resulting in a measuring time per block of 1.0 second. This time is approximately equal to the reverberation time of the barrel volume, accounting for reverberation effects inside the barrel. For each array station, data have been acquired over 60

seconds. With this approach, sufficient high coherence values were obtained between the signal generator output and the array microphones, see Fig. 4.

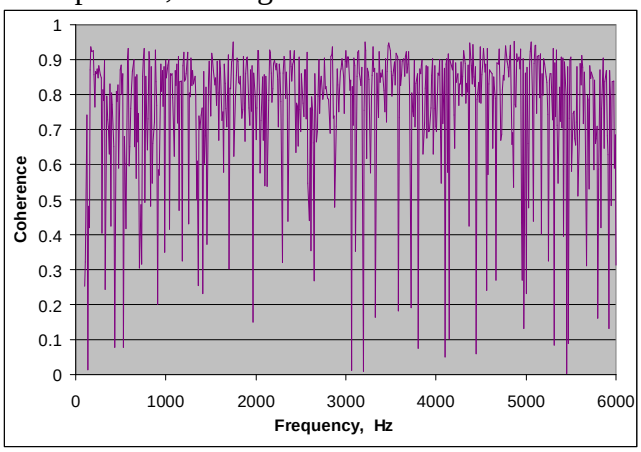

Fig. 4. Typical coherence data between the signal generator output and one of the array microphones

Concerning the ISO 15186(2) TL measurements, the average sound pressure level inside the barrel has been determined from the sound pressures, measured at 8 positions inside the barrel. The average sound intensity over the measuring surface, normal to the barrel surface, has been determined by scanning the measuring surface by hand, at a distance of about 5 cm from the barrel surface.

4 Experimental Results

Fig. 5 shows the TL of the FUBACOMP barrel wall (according to ISO 15186(2) [5]), for two source positions, as determined from the array data, in comparison with the corresponding TL data, determined from the intensity measurements. The two types of TL plots show a very good agreement. From this, it is concluded that the sound pressure and its normal derivative at the fuselage wall can be reconstructed accurately with the NAH method, and that the test set-up is appropriate.

One-third octave band maps of $-TL_R$ ($=20\log\left|TF(q)\cdot S_{ref}\right|$) are plotted in Fig. 6, for source position 1. The presented data are equivalent to the normal pressure derivative at the barrel surface (converted to dB). The values "0" and "1.6" on the horizontal axis of the plots in this figure correspond with axial positions of 46 and 204 cm in front of the grey metal plate at the rear (see Fig. 1).

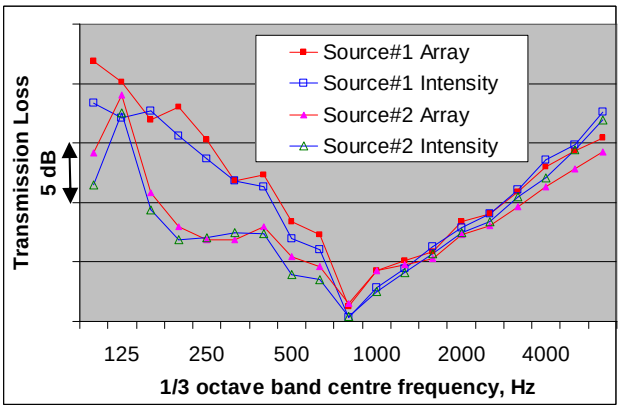

Fig. 5. Results of reciprocal TL measurements, in comparison to the corresponding TL data, determined from the intensity measurements

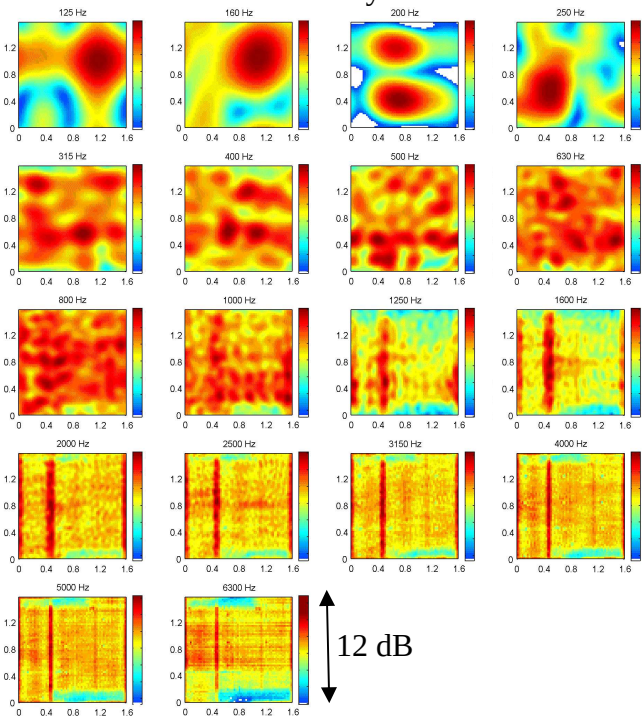

Fig. 6. Maps of $-TL_R$ in dB for source position 1; horizontal = axial, vertical = circumferential position in meters

A remarkable feature is the presence of vertical lines at frequencies above 1000 Hz. These lines, which are along the circumference (i.e. fixed axial positions, in particular at 0.4 m), seem to point at locations with a relatively large sound transmission. The data have been post processed also for array traverses over axial intervals, different from the interval in Fig. 6. In the corresponding results, these lines appeared at

different positions in the plot, but always corresponding with the same axial position on the barrel. For a repeat measurement however, and for the measurement with the source at position 2, these lines did not occur. The reason for this is not yet understood.

Some more observations can be made from Fig. 5. All TL curves in Fig. 5 show a minimum in the 800 Hz 1/3 octave band, which is attributed to the ring frequency. The predicted value of the ring frequency (884 Hz, according to the definition in Ref. [7]) agrees well with the measured value. According to the theory [7], the Fubacomp wall shows a mass law behaviour (as for a flat plate) above the ring frequency, as can be observed in Fig. 5. Below the ring frequency, the sound transmission through the barrel is governed by its membrane stiffness.

In Fig. 5, also the effect of the source position on the TL is shown. For the ring frequency and higher frequencies, the same TL has been measured for both source positions. Below the ring frequency however, different TL values appear for both source positions. These differences are attributed to deviations from a diffuse sound field inside the barrel. In particular for lower frequencies (small mode density), different modes may be excited, depending on the source being located in a node or an antinode.

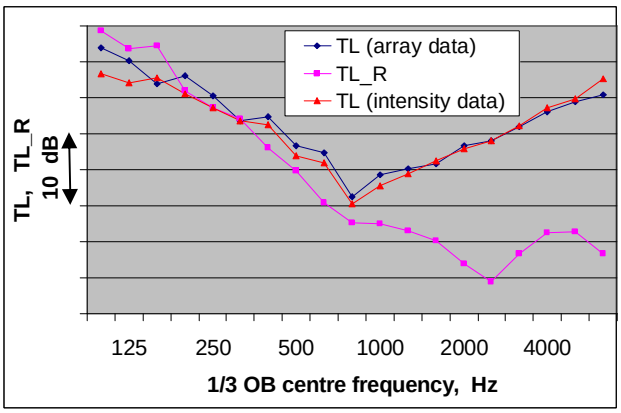

Fig. 7. Barrel wall TL, compared with the corresponding TL_R data

Fig. 7 shows the TL_R data of the barrel surface, averaged over the test surface corresponding with the Fig. 6 maps, and the corresponding TL data, determined both from the array data and the measured sound intensity data. Below the ring frequency there is a fair agreement between TL and TL_R, but for larger frequencies both results diverge. This may be caused by a different sound radiating behaviour of the barrel below and above the ring frequency. Apparently, sound pressure and particle velocity are more in phase (like in a plane wave) for frequencies below the ring frequency, resulting in $I_n \approx \frac{|p|^2}{2\rho_0 c} \approx \frac{|\partial p/\partial n|^2}{2\rho_0 c k^2}$. For frequencies above the ring frequency, this is not the case. It is noted that, if the TL would be measured with the sound source located outside instead of inside the barrel, the TL will approximate the TL_R curve in Fig. 7. This follows from Lyamshev's principle of reciprocity $p_1/f_1 = (-\partial p_2/\partial n)/q_2$ (see Fig. 2).

Also TL measurements have been performed by Dassault on a flat panel (see Fig. 8) fixed between a reverberant room and an anechoic room.

Fig. 8. Dassault set-up for TL measurement of the FUBACOMP panel

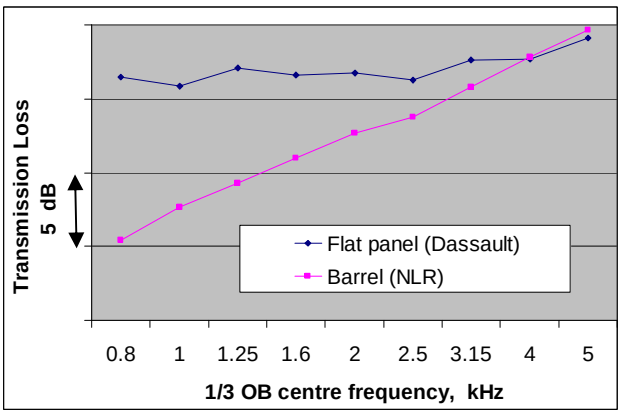

Fig. 9. TL measured on a flat FUBACOMP panel and on the FUBACOMP barrel

The TL was determined according to ISO 15186, from the measured intensity averaged

over the surface of the panel. The measurement bias of the flat panel test rooms has been measured on an aluminium plate and is added to the measurement TL values of the flat panel. The flat panel and barrel TL values, as depicted in Fig. 9, show that the TL measured on the two structures is different, except for the 4 kHz octave band.

This difference is caused mainly by the effect of the ring frequency, dominating the sound transmission behaviour of the barrel, as opposed to that of the flat panel.

5 Conclusions

The sound transmission through a composite business jet fuselage with a honeycomb primary structure, both TL and TL_R, have been determined with a reciprocal technique, determining the exterior sound field with NAH. Also the TL of both the barrel and a flat panel with the same structure has been measured according to ISO 15186. From the experimental results, the following can be concluded.

- TL results obtained with the traversed microphone array agree well with the results of the conventional intensity method, indicating that the NAH technique works well.
- For frequencies below the ring frequency, there is a fair agreement between the measured TL and TL_R data. Above the ring frequency, these data diverge. This is attributed to differences in the vibration behaviour of the barrel below the ring frequency (breathing cylinder) and above it (multiple modes like in a flat plate).
- The TL measured on the barrel and on a flat panel with the same structure deviate from each other, except for the 4 kHz octave band. This difference is attributed mainly to the effect of the ring frequency, dominating the barrel sound transmission behaviour.

6 Acknowledgements

EU is acknowledged for providing part of the funding for the presented work. The FUBACOMP consortium (EU-FP5 programme FUll BArrel COMPosite) is acknowledged for making available the barrel for noise testing, and CEAT for making available one of their test halls in Toulouse.

The NLR colleagues Onno Stallinga, Marko Beenders, Arjan Hanema and Rob Beeldman are acknowledged for their invaluable contributions to the test campaign and the acquisition of the experimental data, Jan Halm for the design and Jack Bijker for the manufacturing of the acoustic array.

7 References

[1] Mason J.M, Fahy F.J. Development of a reciprocity technique for the prediction of propeller noise transmission through aircraft fuselages. *Noise Control Engineering Journal*, Vol. 34, No 2, pp 43-52, 1990.

[2] Fahy F.J, Mason J.M. Measurements of the sound transmission characteristics of model aircraft fuselages using a reciprocity technique. *Noise Control Engineering Journal*, Vol. 37, No 1, pp 19-29, 1991.

[3] MacMartin D.G. Aircraft fuselage noise transmission measurements using a reciprocity technique, *Journal of Sound and Vibration*, Vol. 187, No. 3, pp 467-483, 1995

[4] Williams E.G. *Fourier acoustics*. 1st edition, Academic Press, 1999.

[5] ISO 15186. *Acoustics -- Measurement of sound insulation in buildings and of building elements using sound intensity. -- Part 2: Field measurements*. International Standardization Organization, 2003.

[6] Lyamshev L.M, Theory of sound radiation by thin elastic shells and plates. *Sov. Phys. Acoust.*, Vol. 5, No. 4, pp. 431-438, 1960.

[7] Fahy F.J. *Sound and Structural Vibration; Radiation, Transmission and Response*. 1st edition, Academic Press, 1985.

Copyright Statement